

# Today's outline - April 02, 2020 (part A)

# Today's outline - April 02, 2020 (part A)

- Angle Resolved Photoemission

# Today's outline - April 02, 2020 (part A)

- Angle Resolved Photoemission
- HAXPES

# Today's outline - April 02, 2020 (part A)

- Angle Resolved Photoemission
- HAXPES

Homework Assignment #06:

Chapter 6: 1,6,7,8,9

due Tuesday, April 14, 2020

# Today's outline - April 02, 2020 (part A)

- Angle Resolved Photoemission
- HAXPES

Homework Assignment #06:

Chapter 6: 1,6,7,8,9

due Tuesday, April 14, 2020

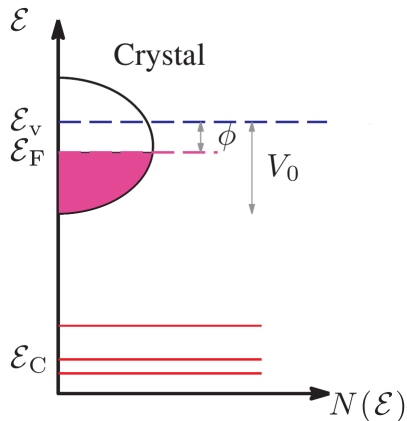
Homework Assignment #07:

Chapter 7: 2,3,9,10,11

due Thursday, April 23, 2020

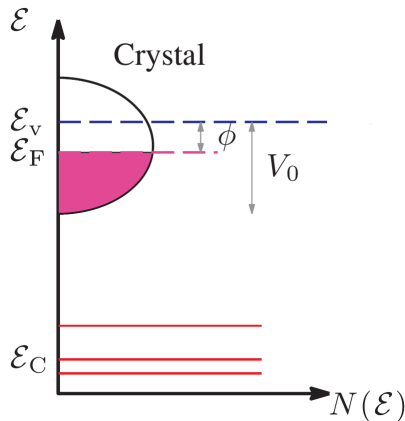
# The photoemission process

Photoemission is the complement to XAFS. It probes the filled states below the Fermi level



# The photoemission process

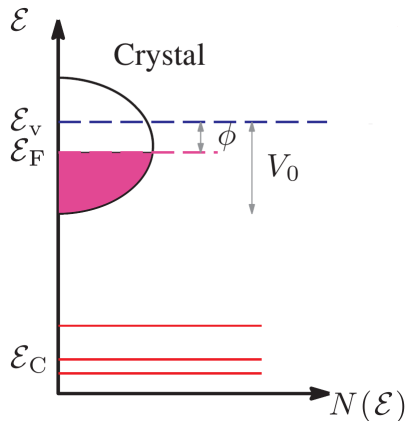
Photoemission is the complement to XAFS. It probes the filled states below the Fermi level



The dispersion relation of electrons in a solid,  $\mathcal{E}(\vec{q})$  can be probed by angle resolved photoemission since both the kinetic energy,  $\mathcal{E}_{kin}$ , and the angle,  $\theta$  are measured

# The photoemission process

Photoemission is the complement to XAFS. It probes the filled states below the Fermi level



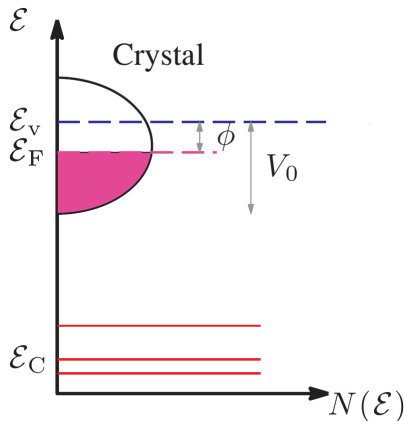
The dispersion relation of electrons in a solid,  $\mathcal{E}(\vec{q})$  can be probed by angle resolved photoemission since both the kinetic energy,  $\mathcal{E}_{kin}$ , and the angle,  $\theta$  are measured

$$\mathcal{E}_{kin}, \theta \longrightarrow \mathcal{E}(\vec{q})$$



# The photoemission process

Photoemission is the complement to XAFS. It probes the filled states below the Fermi level



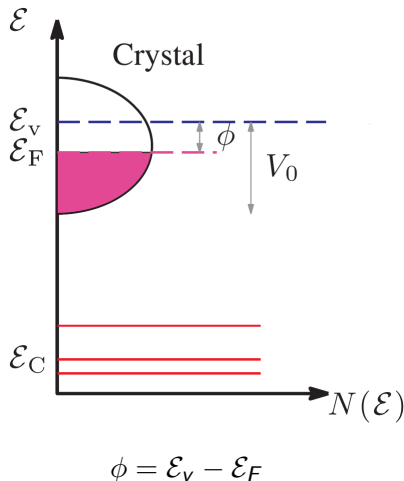
The dispersion relation of electrons in a solid,  $\mathcal{E}(\vec{q})$  can be probed by angle resolved photoemission since both the kinetic energy,  $\mathcal{E}_{kin}$ , and the angle,  $\theta$  are measured

$$\mathcal{E}_{kin}, \theta \rightarrow \mathcal{E}(\vec{q})$$

The core levels are tightly bound at an energy  $\mathcal{E}_C$  below the Fermi level

# The photoemission process

Photoemission is the complement to XAFS. It probes the filled states below the Fermi level



The dispersion relation of electrons in a solid,  $\mathcal{E}(\vec{q})$  can be probed by angle resolved photoemission since both the kinetic energy,  $\mathcal{E}_{kin}$ , and the angle,  $\theta$  are measured

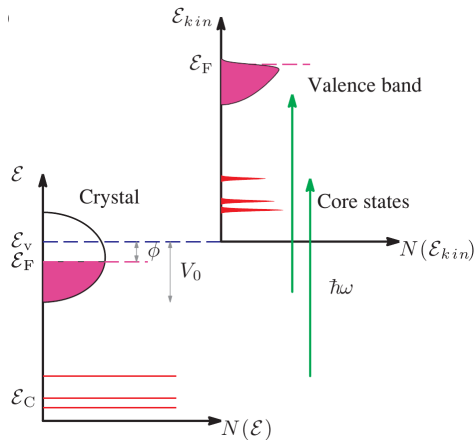
$$\mathcal{E}_{kin}, \theta \rightarrow \mathcal{E}(\vec{q})$$

The core levels are tightly bound at an energy  $\mathcal{E}_C$  below the Fermi level

The work function,  $\phi$ , is the minimum energy required to promote an electron from the top of the valence band at the Fermi energy,  $\mathcal{E}_F$ , to the vacuum energy,  $\mathcal{E}_v$

# The photoemission process

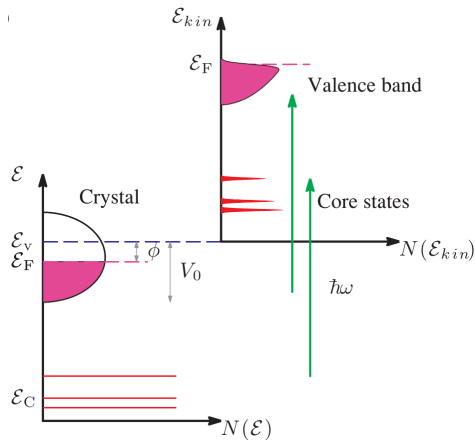
With the incident photon energy,  $\hbar\omega$ , held constant, an analyzer is used to measure the kinetic energy,  $\mathcal{E}_{kin}$ , of the photoelectrons emitted from the surface of the sample



# The photoemission process

With the incident photon energy,  $\hbar\omega$ , held constant, an analyzer is used to measure the kinetic energy,  $\mathcal{E}_{kin}$ , of the photoelectrons emitted from the surface of the sample

if  $\mathcal{E}_i$  is the initial energy of the electron, the binding energy,  $\mathcal{E}_B$  is

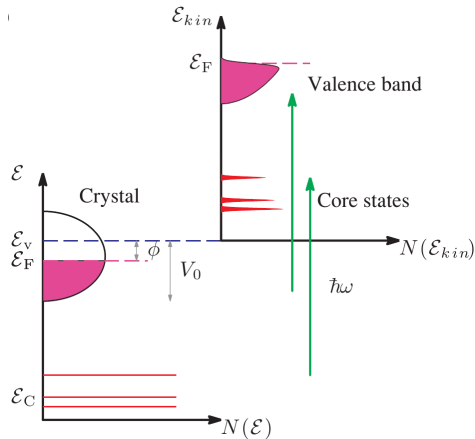


# The photoemission process

With the incident photon energy,  $\hbar\omega$ , held constant, an analyzer is used to measure the kinetic energy,  $\mathcal{E}_{kin}$ , of the photoelectrons emitted from the surface of the sample

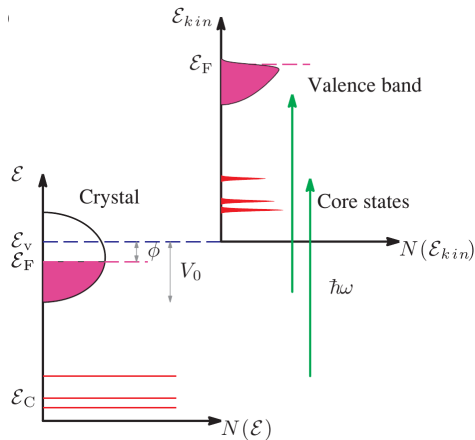
if  $\mathcal{E}_i$  is the initial energy of the electron, the binding energy,  $\mathcal{E}_B$  is

$$\mathcal{E}_B = \mathcal{E}_F - \mathcal{E}_i$$



# The photoemission process

With the incident photon energy,  $\hbar\omega$ , held constant, an analyzer is used to measure the kinetic energy,  $\mathcal{E}_{kin}$ , of the photoelectrons emitted from the surface of the sample



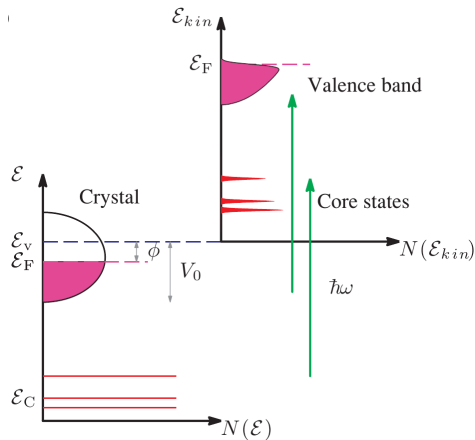
if  $\mathcal{E}_i$  is the initial energy of the electron, the binding energy,  $\mathcal{E}_B$  is

$$\mathcal{E}_B = \mathcal{E}_F - \mathcal{E}_i$$

and the measured kinetic energy gives the binding energy

# The photoemission process

With the incident photon energy,  $\hbar\omega$ , held constant, an analyzer is used to measure the kinetic energy,  $\mathcal{E}_{kin}$ , of the photoelectrons emitted from the surface of the sample



if  $\mathcal{E}_i$  is the initial energy of the electron, the binding energy,  $\mathcal{E}_B$  is

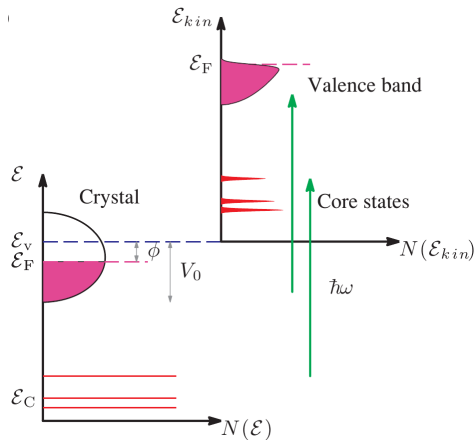
$$\mathcal{E}_B = \mathcal{E}_F - \mathcal{E}_i$$

and the measured kinetic energy gives the binding energy

$$\mathcal{E}_{kin} = \frac{\hbar^2 q_v^2}{2m}$$

# The photoemission process

With the incident photon energy,  $\hbar\omega$ , held constant, an analyzer is used to measure the kinetic energy,  $\mathcal{E}_{kin}$ , of the photoelectrons emitted from the surface of the sample



if  $\mathcal{E}_i$  is the initial energy of the electron, the binding energy,  $\mathcal{E}_B$  is

$$\mathcal{E}_B = \mathcal{E}_F - \mathcal{E}_i$$

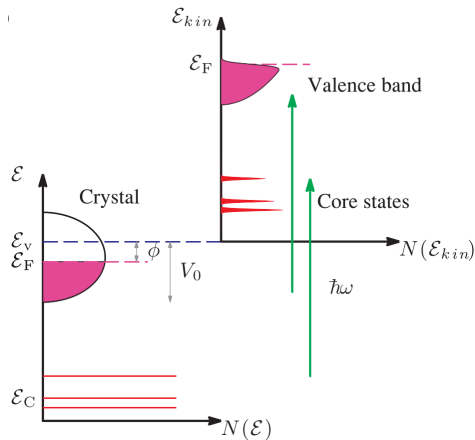
and the measured kinetic energy gives the binding energy

$$\mathcal{E}_{kin} = \frac{\hbar^2 q_v^2}{2m} = \hbar\omega - \phi - \mathcal{E}_B$$



# The photoemission process

With the incident photon energy,  $\hbar\omega$ , held constant, an analyzer is used to measure the kinetic energy,  $\mathcal{E}_{kin}$ , of the photoelectrons emitted from the surface of the sample



if  $\mathcal{E}_i$  is the initial energy of the electron, the binding energy,  $\mathcal{E}_B$  is

$$\mathcal{E}_B = \mathcal{E}_F - \mathcal{E}_i$$

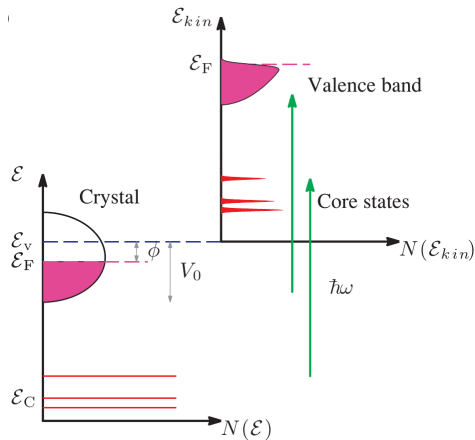
and the measured kinetic energy gives the binding energy

$$\mathcal{E}_{kin} = \frac{\hbar^2 q_v^2}{2m} = \hbar\omega - \phi - \mathcal{E}_B$$

the maximum kinetic energy measured is thus related to the Fermi energy

# The photoemission process

With the incident photon energy,  $\hbar\omega$ , held constant, an analyzer is used to measure the kinetic energy,  $\mathcal{E}_{kin}$ , of the photoelectrons emitted from the surface of the sample



if  $\mathcal{E}_i$  is the initial energy of the electron, the binding energy,  $\mathcal{E}_B$  is

$$\mathcal{E}_B = \mathcal{E}_F - \mathcal{E}_i$$

and the measured kinetic energy gives the binding energy

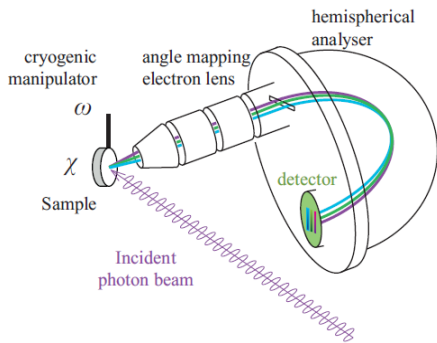
$$\mathcal{E}_{kin} = \frac{\hbar^2 q_v^2}{2m} = \hbar\omega - \phi - \mathcal{E}_B$$

the maximum kinetic energy measured is thus related to the Fermi energy

the core states are used to fingerprint the chemical composition of the sample

# Hemispherical mirror analyzer

The electric field between the two hemispheres of radius  $R_1$  and  $R_2$  has a  $R^2$  dependence from the center of the hemispheres

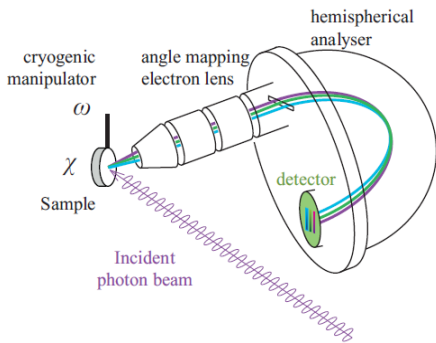


# Hemispherical mirror analyzer

The electric field between the two hemispheres of radius  $R_1$  and  $R_2$  has a  $R^2$  dependence from the center of the hemispheres

Electrons with  $\mathcal{E}_0$ , called the “pass energy”, will follow a circular path of radius

$$R_0 = (R_1 + R_2)/2$$

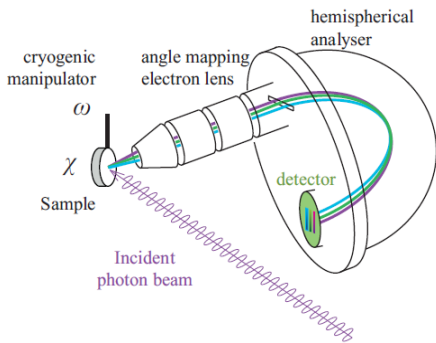


# Hemispherical mirror analyzer

The electric field between the two hemispheres of radius  $R_1$  and  $R_2$  has a  $R^2$  dependence from the center of the hemispheres

Electrons with  $\mathcal{E}_0$ , called the “pass energy”, will follow a circular path of radius

$$R_0 = (R_1 + R_2)/2$$



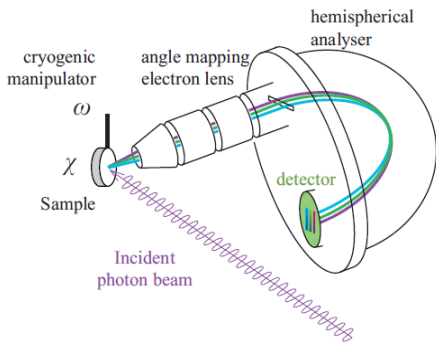
# Hemispherical mirror analyzer

The electric field between the two hemispheres of radius  $R_1$  and  $R_2$  has a  $R^2$  dependence from the center of the hemispheres

Electrons with  $\mathcal{E}_0$ , called the “pass energy”, will follow a circular path of radius

$$R_0 = (R_1 + R_2)/2$$

Electrons with lower energy will fall inside this circular path while those with higher energy will fall outside



# Hemispherical mirror analyzer

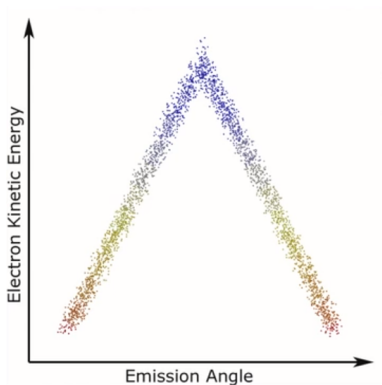
The electric field between the two hemispheres of radius  $R_1$  and  $R_2$  has a  $R^2$  dependence from the center of the hemispheres

Electrons with  $\mathcal{E}_0$ , called the “pass energy”, will follow a circular path of radius

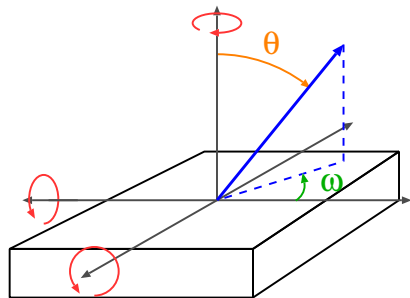
$$R_0 = (R_1 + R_2)/2$$

Electrons with lower energy will fall inside this circular path while those with higher energy will fall outside

Electrons with different azimuthal exit angles  $\omega$  will map to different positions on the 2D detector



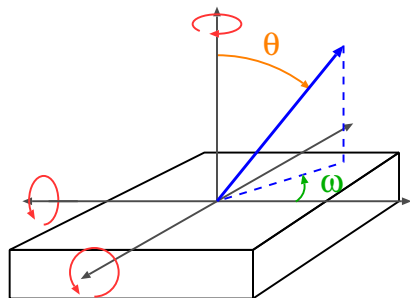
# Photoelectron momentum





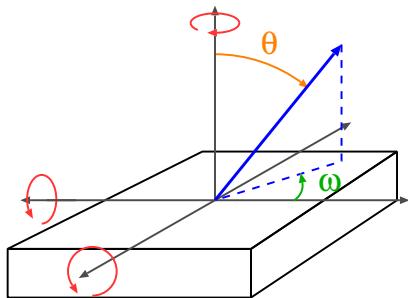
# Photoelectron momentum

The total **momentum** of the photoelectron is calculated from the measured kinetic energy



# Photoelectron momentum

The total **momentum** of the photoelectron is calculated from the measured kinetic energy

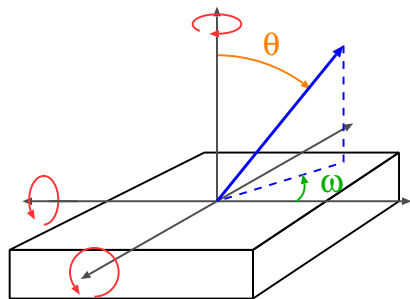


$$\hbar q_e = \sqrt{2m\mathcal{E}_{kin}}$$

# Photoelectron momentum

The total **momentum** of the photoelectron is calculated from the measured kinetic energy

since the momentum of the electron parallel to the surface must be conserved, the original momentum of the electron can be computed from the **polar angle** of the sample to the detector and the **azimuthal angle** measured on the 2D detector

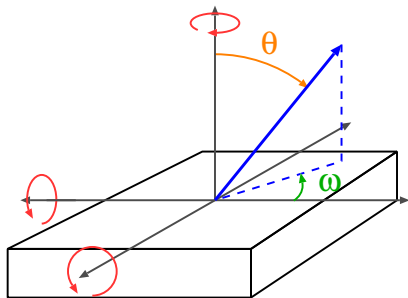


$$\hbar q_e = \sqrt{2m\mathcal{E}_{kin}}$$

# Photoelectron momentum

The total momentum of the photoelectron is calculated from the measured kinetic energy

since the momentum of the electron parallel to the surface must be conserved, the original momentum of the electron can be computed from the polar angle of the sample to the detector and the azimuthal angle measured on the 2D detector



$$\hbar q_e = \sqrt{2m\mathcal{E}_{kin}}$$

$$\hbar q_{\parallel x} = \hbar q_e \sin \theta \cos \omega$$

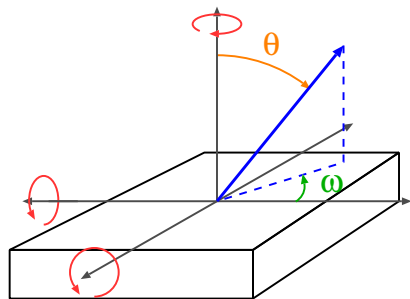
$$\hbar q_{\parallel y} = \hbar q_e \sin \theta \sin \omega$$

# Photoelectron momentum

The total **momentum** of the photoelectron is calculated from the measured kinetic energy

since the momentum of the electron parallel to the surface must be conserved, the original momentum of the electron can be computed from the **polar angle** of the sample to the detector and the **azimuthal angle** measured on the 2D detector

the perpendicular component of the original momentum can be obtained by assuming a free electron and measuring the inner potential,  $V_0$  at  $\theta = 0$



$$\hbar q_e = \sqrt{2m\mathcal{E}_{kin}}$$

$$\hbar q_{\parallel x} = \hbar q_e \sin \theta \cos \omega$$

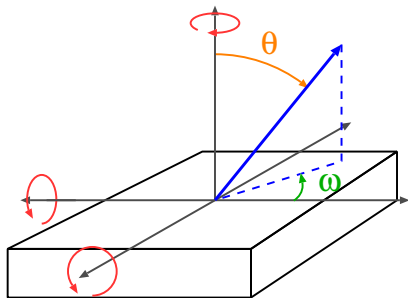
$$\hbar q_{\parallel y} = \hbar q_e \sin \theta \sin \omega$$

# Photoelectron momentum

The total **momentum** of the photoelectron is calculated from the measured kinetic energy

since the momentum of the electron parallel to the surface must be conserved, the original momentum of the electron can be computed from the **polar angle** of the sample to the detector and the **azimuthal angle** measured on the 2D detector

the perpendicular component of the original momentum can be obtained by assuming a free electron and measuring the inner potential,  $V_0$  at  $\theta = 0$



$$\hbar q_e = \sqrt{2m\mathcal{E}_{kin}}$$

$$\hbar q_{\parallel x} = \hbar q_e \sin \theta \cos \omega$$

$$\hbar q_{\parallel y} = \hbar q_e \sin \theta \sin \omega$$

$$\hbar q_{\perp} = \sqrt{2m(\mathcal{E}_{kin} \cos^2 \theta + V_0)}$$

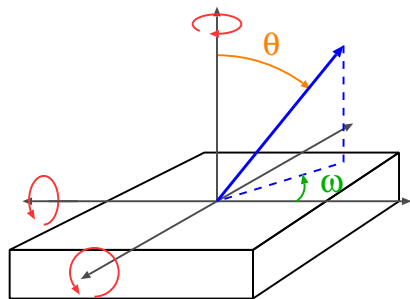
# Photoelectron momentum

The total momentum of the photoelectron is calculated from the measured kinetic energy

since the momentum of the electron parallel to the surface must be conserved, the original momentum of the electron can be computed from the polar angle of the sample to the detector and the azimuthal angle measured on the 2D detector

the perpendicular component of the original momentum can be obtained by assuming a free electron and measuring the inner potential,  $V_0$  at  $\theta = 0$

the electron dispersion curve can be fully mapped by sample rotations



$$\hbar q_e = \sqrt{2m\mathcal{E}_{kin}}$$

$$\hbar q_{\parallel x} = \hbar q_e \sin \theta \cos \omega$$

$$\hbar q_{\parallel y} = \hbar q_e \sin \theta \sin \omega$$

$$\hbar q_{\perp} = \sqrt{2m(\mathcal{E}_{kin} \cos^2 \theta + V_0)}$$

# HAXPES

Photoemission spectroscopy is generally used for surface sensitive measurements because of the low energy of the incident photons ( $< 2$  keV)



# HAXPES

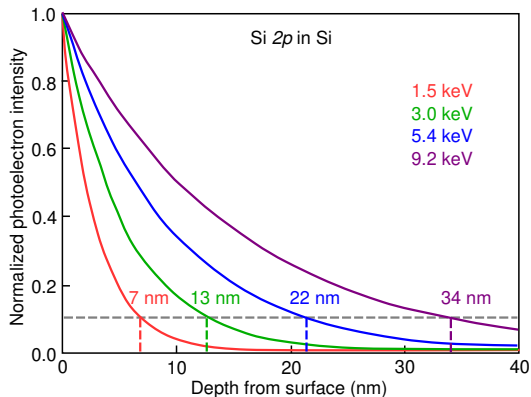
Photoemission spectroscopy is generally used for surface sensitive measurements because of the low energy of the incident photons ( $< 2$  keV)

High energy synchrotrons offer the opportunity to use hard x-ray photoelectron spectroscopy (HAXPES)

# HAXPES

Photoemission spectroscopy is generally used for surface sensitive measurements because of the low energy of the incident photons ( $< 2$  keV)

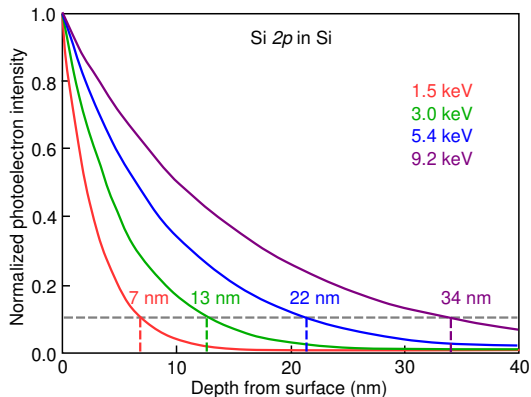
High energy synchrotrons offer the opportunity to use hard x-ray photoelectron spectroscopy (HAXPES)



# HAXPES

Photoemission spectroscopy is generally used for surface sensitive measurements because of the low energy of the incident photons ( $< 2$  keV)

High energy synchrotrons offer the opportunity to use hard x-ray photoelectron spectroscopy (HAXPES)

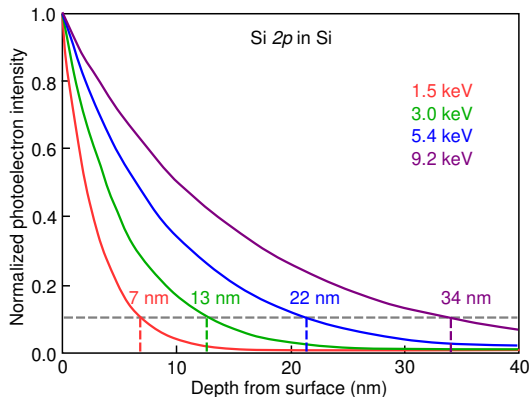


HAXPES advantages include

# HAXPES

Photoemission spectroscopy is generally used for surface sensitive measurements because of the low energy of the incident photons ( $< 2$  keV)

High energy synchrotrons offer the opportunity to use hard x-ray photoelectron spectroscopy (HAXPES)

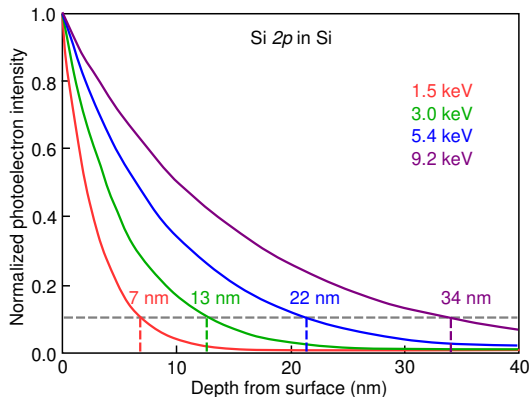


HAXPES advantages include measurement of K edges of 3d elements, L edges of 5d elements, and M edges of 5f elements

# HAXPES

Photoemission spectroscopy is generally used for surface sensitive measurements because of the low energy of the incident photons ( $< 2$  keV)

High energy synchrotrons offer the opportunity to use hard x-ray photoelectron spectroscopy (HAXPES)



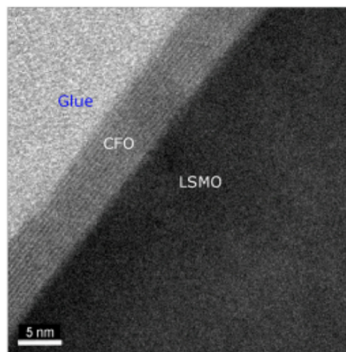
HAXPES advantages include

measurement of K edges of 3d elements, L edges of 5d elements, and M edges of 5f elements

ability to measure bulk photoemission and buried interfaces as well as the surface

## HAXPES of buried interfaces

HAXPES is used to probe the thickness of a  $\text{CoFe}_2\text{O}_4/\text{La}_{0.66}\text{Sr}_{0.34}\text{MnO}_3$  heterostructure by varying both angle of incidence and photon energy

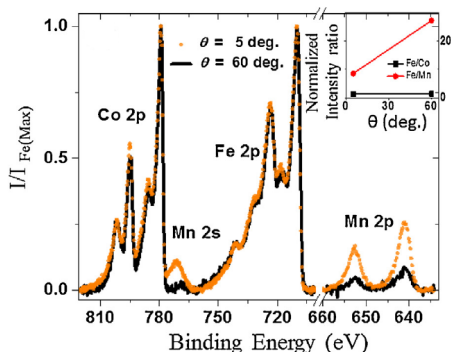


The thickness of the  $\text{CoFe}_2\text{O}_4$  overlayer measured as  $6.5 \pm 0.5$  nm by TEM was probed in two ways:

B. Pal, S. Mukherjee, and D.D. Sarma, "Probing complex heterostructures using hard x-ray photoelectron spectroscopy (HAXPES)," *J. Electron Spect. Related Phenomena* **200**, 332-339 (2015).

# HAXPES of buried interfaces

HAXPES is used to probe the thickness of a  $\text{CoFe}_2\text{O}_4/\text{La}_{0.66}\text{Sr}_{0.34}\text{MnO}_3$  heterostructure by varying both angle of incidence and photon energy



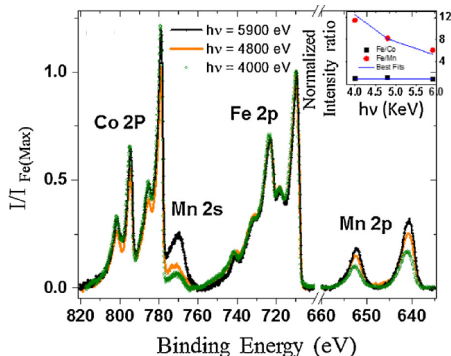
The thickness of the  $\text{CoFe}_2\text{O}_4$  over-layer measured as  $6.5 \pm 0.5$  nm by TEM was probed in two ways:

using 4.8 keV photons and varying the angle, the thickness is estimated to be  $8.0 \pm 2.0$  nm

B. Pal, S. Mukherjee, and D.D. Sarma, "Probing complex heterostructures using hard x-ray photoelectron spectroscopy (HAXPES)," *J. Electron Spect. Related Phenomena* **200**, 332-339 (2015).

# HAXPES of buried interfaces

HAXPES is used to probe the thickness of a  $\text{CoFe}_2\text{O}_4/\text{La}_{0.66}\text{Sr}_{0.34}\text{MnO}_3$  heterostructure by varying both angle of incidence and photon energy



The thickness of the  $\text{CoFe}_2\text{O}_4$  over-layer measured as  $6.5 \pm 0.5$  nm by TEM was probed in two ways:

using 4.8 keV photons and varying the angle, the thickness is estimated to be  $8.0 \pm 2.0$  nm

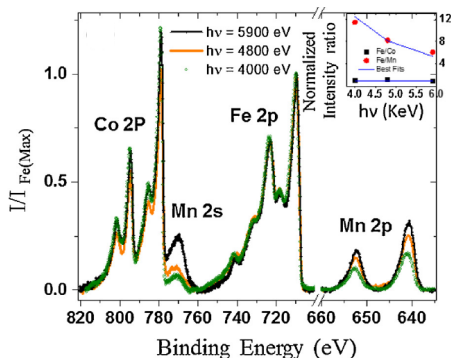
using photon energies from 4.0 keV to 6.0 keV, the thickness was estimated to be  $6.8 \pm 2.8$  nm

B. Pal, S. Mukherjee, and D.D. Sarma, "Probing complex heterostructures using hard x-ray photoelectron spectroscopy (HAXPES)," *J. Electron Spect. Related Phenomena* **200**, 332-339 (2015).



# HAXPES of buried interfaces

HAXPES is used to probe the thickness of a  $\text{CoFe}_2\text{O}_4/\text{La}_{0.66}\text{Sr}_{0.34}\text{MnO}_3$  heterostructure by varying both angle of incidence and photon energy



The thickness of the  $\text{CoFe}_2\text{O}_4$  overlayer measured as  $6.5 \pm 0.5$  nm by TEM was probed in two ways:

using 4.8 keV photons and varying the angle, the thickness is estimated to be  $8.0 \pm 2.0$  nm

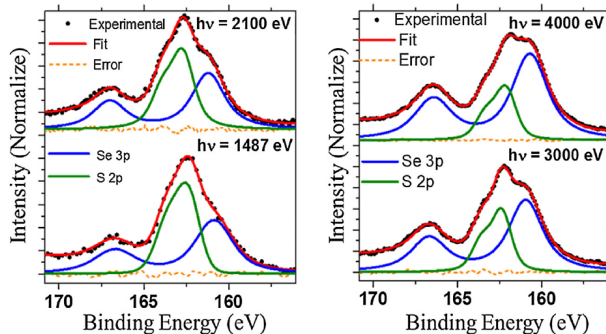
using photon energies from 4.0 keV to 6.0 keV, the thickness was estimated to be  $6.8 \pm 2.8$  nm

Both results give consistent results with proper normalization and also show the uniformity of the  $\text{CoFe}_2\text{O}_4$  overlayer

B. Pal, S. Mukherjee, and D.D. Sarma, "Probing complex heterostructures using hard x-ray photoelectron spectroscopy (HAXPES)," *J. Electron Spect. Related Phenomena* **200**, 332-339 (2015).

# HAXPES of $\text{Zn}_{1-x}\text{Cd}_x\text{Se}_{1-y}\text{S}_y$ nanocrystals

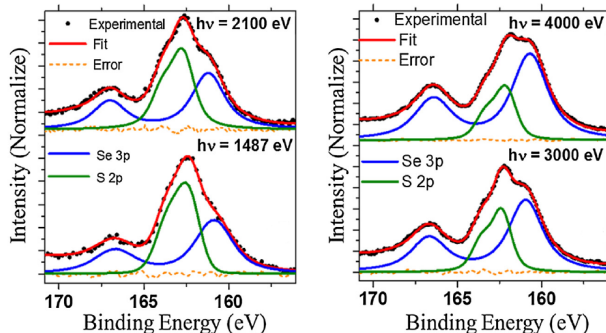
With nanoparticles, energy dispersive measurements can provide depth profiling of spherical nanoparticles



B. Pal, S. Mukherjee, and D.D. Sarma, "Probing complex heterostructures using hard x-ray photoelectron spectroscopy (HAXPES)," *J. Electron Spect. Related Phenomena* **200**, 332-339 (2015).

# HAXPES of $Zn_{1-x}Cd_xSe_{1-y}S_y$ nanocrystals

With nanoparticles, energy dispersive measurements can provide depth profiling of spherical nanoparticles

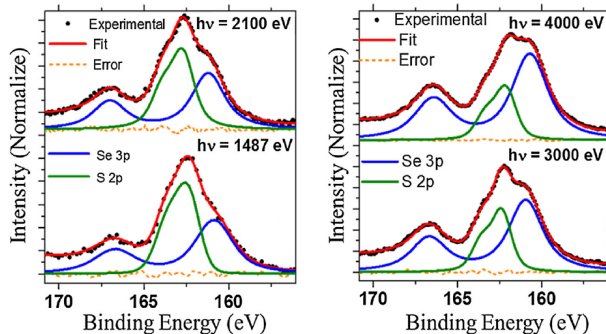


HAXPES at energies ranging from 1.4 keV to 3.0 keV are used to probe the S/Se ratio at varying depths of the 5 nm diameter nanoparticles

B. Pal, S. Mukherjee, and D.D. Sarma, "Probing complex heterostructures using hard x-ray photoelectron spectroscopy (HAXPES)," *J. Electron Spect. Related Phenomena* **200**, 332-339 (2015).

# HAXPES of $\text{Zn}_{1-x}\text{Cd}_x\text{Se}_{1-y}\text{S}_y$ nanocrystals

With nanoparticles, energy dispersive measurements can provide depth profiling of spherical nanoparticles

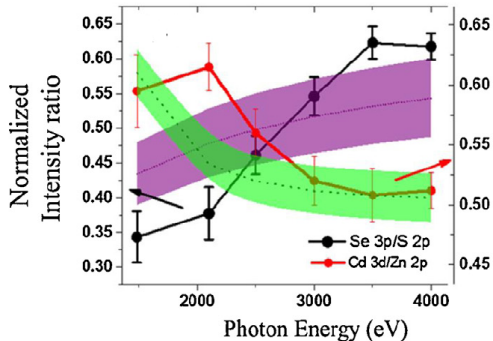


HAXPES at energies ranging from 1.4 keV to 3.0 keV are used to probe the S/Se ratio at varying depths of the 5 nm diameter nanoparticles

By fitting the S 2p and Se 3p photoemission line the structure is revealed to be CdSe at the core and ZnCdS in the outer shell

B. Pal, S. Mukherjee, and D.D. Sarma, "Probing complex heterostructures using hard x-ray photoelectron spectroscopy (HAXPES)," *J. Electron Spect. Related Phenomena* **200**, 332-339 (2015).

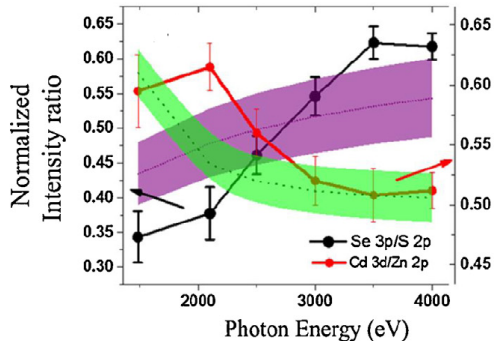
# HAXPES of $\text{Zn}_{1-x}\text{Cd}_x\text{Se}_{1-y}\text{S}_y$ nanocrystals



The variation in intensity of the Se/S lines and the Zn/Cd lines suggest that the Se is primarily located in the 2 nm core of the 5 nm particles with the Cd

B. Pal, S. Mukherjee, and D.D. Sarma, "Probing complex heterostructures using hard x-ray photoelectron spectroscopy (HAXPES)," *J. Electron Spect. Related Phenomena* **200**, 332-339 (2015).

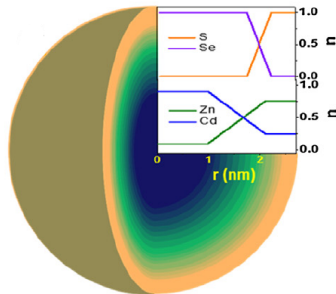
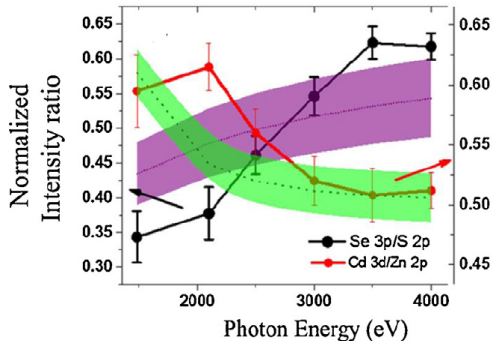
# HAXPES of $Zn_{1-x}Cd_xSe_{1-y}S_y$ nanocrystals



The variation in intensity of the Se/S lines and the Zn/Cd lines suggest that the Se is primarily located in the 2 nm core of the 5 nm particles with the Cd

B. Pal, S. Mukherjee, and D.D. Sarma, "Probing complex heterostructures using hard x-ray photoelectron spectroscopy (HAXPES)," *J. Electron Spect. Related Phenomena* **200**, 332-339 (2015).

# HAXPES of $\text{Zn}_{1-x}\text{Cd}_x\text{Se}_{1-y}\text{S}_y$ nanocrystals



The variation in intensity of the Se/S lines and the Zn/Cd lines suggest that the Se is primarily located in the 2 nm core of the 5 nm particles with the Cd and that there is a graded composition region between the CdSe core and the outer ZnCdS shell

B. Pal, S. Mukherjee, and D.D. Sarma, "Probing complex heterostructures using hard x-ray photoelectron spectroscopy (HAXPES)," *J. Electron Spect. Related Phenomena* **200**, 332-339 (2015).

## HAXPES of Si anodes

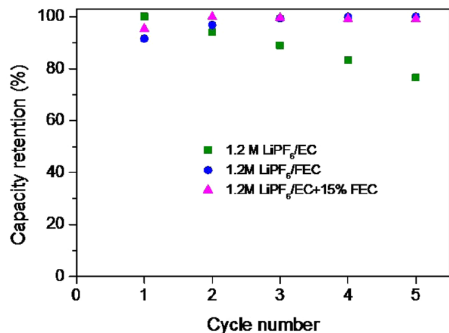
Si nanoparticle anodes suffer from the accumulation of the SEI layer which reduces performance. The SEI is formed by electrochemical decomposition of the electrolyte at the anode surface.

B.T. Young, et al., "Hard x-ray photoelectron spectroscopy (HAXPES) investigation of the silicon solid electrolyte interphase (SEI) in lithium-ion batteries," *ACS Appl. Mater. Interfaces* **7**, 20004-20011 (2015).



# HAXPES of Si anodes

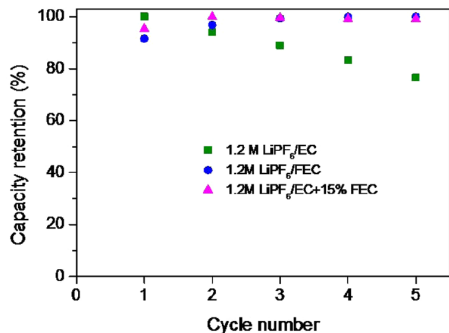
Si nanoparticle anodes suffer from the accumulation of the SEI layer which reduces performance. The SEI is formed by electrochemical decomposition of the electrolyte at the anode surface.



B.T. Young, et al., "Hard x-ray photoelectron spectroscopy (HAXPES) investigation of the silicon solid electrolyte interphase (SEI) in lithium-ion batteries," *ACS Appl. Mater. Interfaces* **7**, 20004-20011 (2015).

# HAXPES of Si anodes

Si nanoparticle anodes suffer from the accumulation of the SEI layer which reduces performance. The SEI is formed by electrochemical decomposition of the electrolyte at the anode surface.

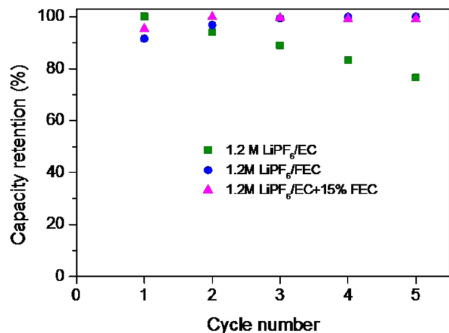


The SEI from three different electrolyte combinations were studied: ethylene carbonate (EC), fluoroethylene carbonate (FEC), and a combination. The first of which gives poorer capacity and cycling stability.

B.T. Young, et al., "Hard x-ray photoelectron spectroscopy (HAXPES) investigation of the silicon solid electrolyte interphase (SEI) in lithium-ion batteries," *ACS Appl. Mater. Interfaces* **7**, 20004-20011 (2015).

# HAXPES of Si anodes

Si nanoparticle anodes suffer from the accumulation of the SEI layer which reduces performance. The SEI is formed by electrochemical decomposition of the electrolyte at the anode surface.

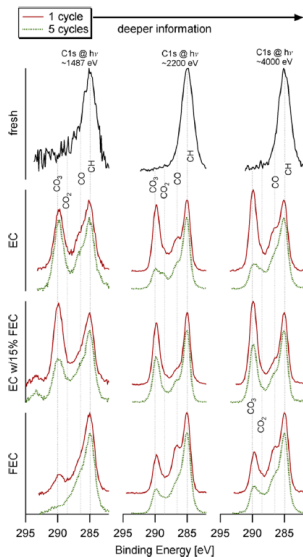


The SEI from three different electrolyte combinations were studied: ethylene carbonate (EC), fluoroethylene carbonate (FEC), and a combination. The first of which gives poorer capacity and cycling stability.

HAXPES is used to determine the elemental distribution and compounds present as a function of depth in the cycled Si anode.

B.T. Young, et al., "Hard x-ray photoelectron spectroscopy (HAXPES) investigation of the silicon solid electrolyte interphase (SEI) in lithium-ion batteries," *ACS Appl. Mater. Interfaces* **7**, 20004-20011 (2015).

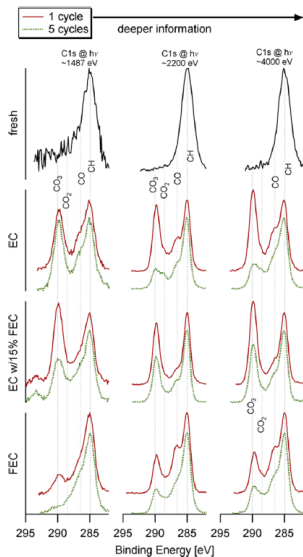
# HAXPES of Si anodes



By varying the incident photon energy, it is possible to probe the SEI as a function of depth.

B.T. Young, et al., "Hard x-ray photoelectron spectroscopy (HAXPES) investigation of the silicon solid electrolyte interphase (SEI) in lithium-ion batteries," *ACS Appl. Mater. Interfaces* **7**, 20004-20011 (2015).

# HAXPES of Si anodes

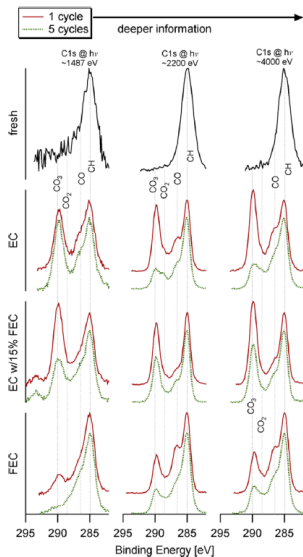


By varying the incident photon energy, it is possible to probe the SEI as a function of depth.

From the carbon peaks, it is seen that:

B.T. Young, et al., "Hard x-ray photoelectron spectroscopy (HAXPES) investigation of the silicon solid electrolyte interphase (SEI) in lithium-ion batteries," *ACS Appl. Mater. Interfaces* 7, 20004-20011 (2015).

# HAXPES of Si anodes



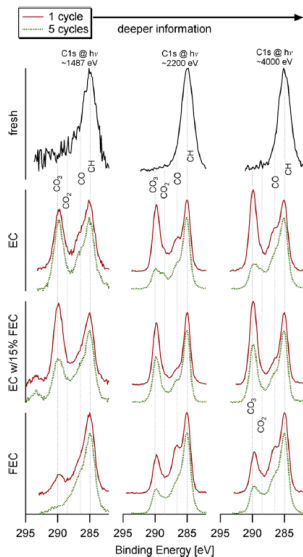
By varying the incident photon energy, it is possible to probe the SEI as a function of depth.

From the carbon peaks, it is seen that:

- increase in carbon concentration is SEI

B.T. Young, et al., "Hard x-ray photoelectron spectroscopy (HAXPES) investigation of the silicon solid electrolyte interphase (SEI) in lithium-ion batteries," *ACS Appl. Mater. Interfaces* **7**, 20004-20011 (2015).

# HAXPES of Si anodes



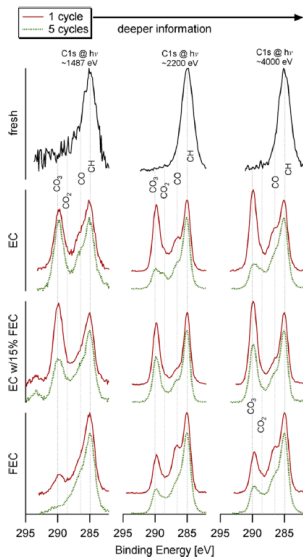
By varying the incident photon energy, it is possible to probe the SEI as a function of depth.

From the carbon peaks, it is seen that:

- increase in carbon concentration is SEI
- SEI visible after first cycle with EC is likely LEDC (290 eV peak)

B.T. Young, et al., "Hard x-ray photoelectron spectroscopy (HAXPES) investigation of the silicon solid electrolyte interphase (SEI) in lithium-ion batteries," *ACS Appl. Mater. Interfaces* 7, 20004-20011 (2015).

# HAXPES of Si anodes



By varying the incident photon energy, it is possible to probe the SEI as a function of depth.

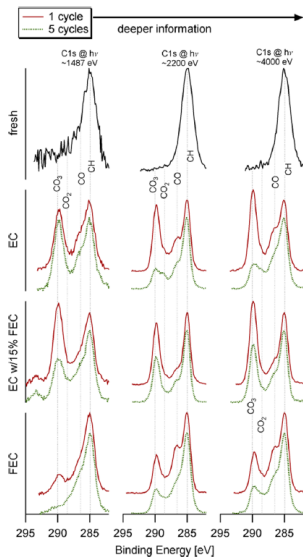
From the carbon peaks, it is seen that:

- increase in carbon concentration is SEI
- SEI visible after first cycle with EC is likely LEDC (290 eV peak)
- after 5 cycles, buried LEDC decomposes in EC electrolytes

B.T. Young, et al., "Hard x-ray photoelectron spectroscopy (HAXPES) investigation of the silicon solid electrolyte interphase (SEI) in lithium-ion batteries," *ACS Appl. Mater. Interfaces* 7, 20004-20011 (2015).



# HAXPES of Si anodes



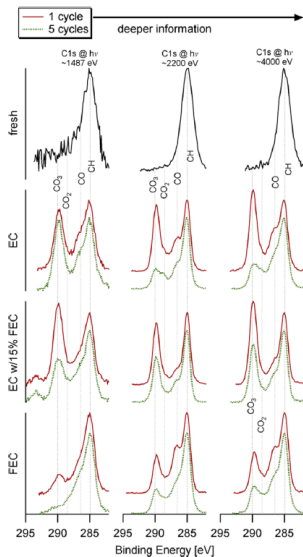
By varying the incident photon energy, it is possible to probe the SEI as a function of depth.

From the carbon peaks, it is seen that:

- increase in carbon concentration is SEI
- SEI visible after first cycle with EC is likely LEDC (290 eV peak)
- after 5 cycles, buried LEDC decomposes in EC electrolytes
- pure FEC shows little LEDC

B.T. Young, et al., "Hard x-ray photoelectron spectroscopy (HAXPES) investigation of the silicon solid electrolyte interphase (SEI) in lithium-ion batteries," *ACS Appl. Mater. Interfaces* 7, 20004-20011 (2015).

# HAXPES of Si anodes



By varying the incident photon energy, it is possible to probe the SEI as a function of depth.

From the carbon peaks, it is seen that:

- increase in carbon concentration is SEI
- SEI visible after first cycle with EC is likely LEDC (290 eV peak)
- after 5 cycles, buried LEDC decomposes in EC electrolytes
- pure FEC shows little LEDC
- pure FEC shows less change with cycling than EC containing electrolytes

B.T. Young, et al., "Hard x-ray photoelectron spectroscopy (HAXPES) investigation of the silicon solid electrolyte interphase (SEI) in lithium-ion batteries," *ACS Appl. Mater. Interfaces* 7, 20004-20011 (2015).

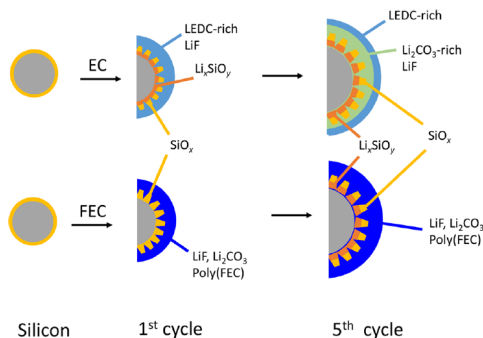
# HAXPES of Si anodes

Using HAXPES data from Si, C, and F, a picture of SEI evolution dependence on electrolyte emerges

B.T. Young, et al., "Hard x-ray photoelectron spectroscopy (HAXPES) investigation of the silicon solid electrolyte interphase (SEI) in lithium-ion batteries," *ACS Appl. Mater. Interfaces* **7**, 20004-20011 (2015).

# HAXPES of Si anodes

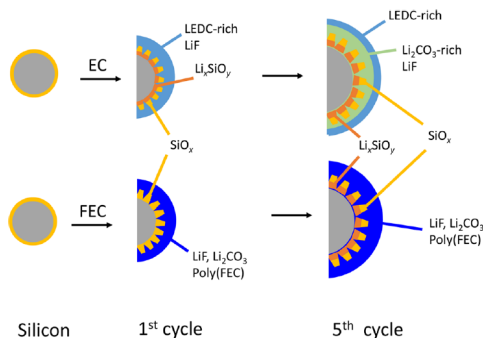
Using HAXPES data from Si, C, and F, a picture of SEI evolution dependence on electrolyte emerges



B.T. Young, et al., "Hard x-ray photoelectron spectroscopy (HAXPES) investigation of the silicon solid electrolyte interphase (SEI) in lithium-ion batteries," *ACS Appl. Mater. Interfaces* **7**, 20004-20011 (2015).

# HAXPES of Si anodes

Using HAXPES data from Si, C, and F, a picture of SEI evolution dependence on electrolyte emerges

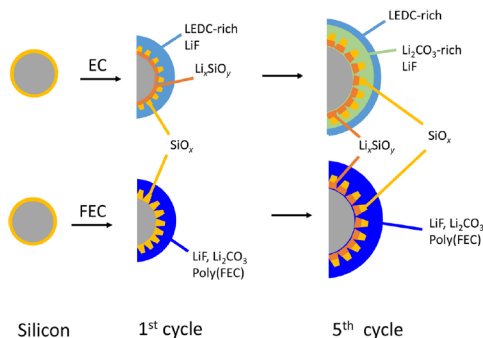


as SEI grows, there is growth of  $\text{Li}_x\text{SiO}_y$  underneath as product of lithiation/delithiation

B.T. Young, et al., "Hard x-ray photoelectron spectroscopy (HAXPES) investigation of the silicon solid electrolyte interphase (SEI) in lithium-ion batteries," *ACS Appl. Mater. Interfaces* **7**, 20004-20011 (2015).

# HAXPES of Si anodes

Using HAXPES data from Si, C, and F, a picture of SEI evolution dependence on electrolyte emerges



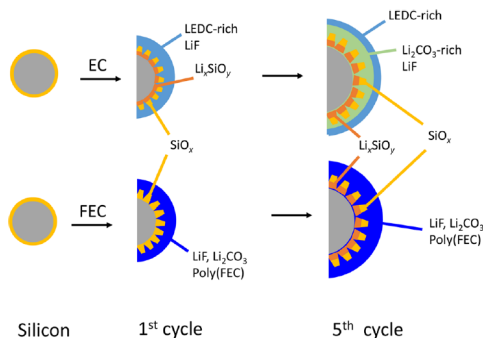
as SEI grows, there is growth of  $\text{Li}_x\text{SiO}_y$  underneath as product of lithiation/delithiation

EC – SEI contains LEDC-rich SEI which decomposes but continues to be deposited with cycling

B.T. Young, et al., "Hard x-ray photoelectron spectroscopy (HAXPES) investigation of the silicon solid electrolyte interphase (SEI) in lithium-ion batteries," *ACS Appl. Mater. Interfaces* **7**, 20004-20011 (2015).

# HAXPES of Si anodes

Using HAXPES data from Si, C, and F, a picture of SEI evolution dependence on electrolyte emerges



as SEI grows, there is growth of  $\text{Li}_x\text{SiO}_y$  underneath as product of lithiation/delithiation

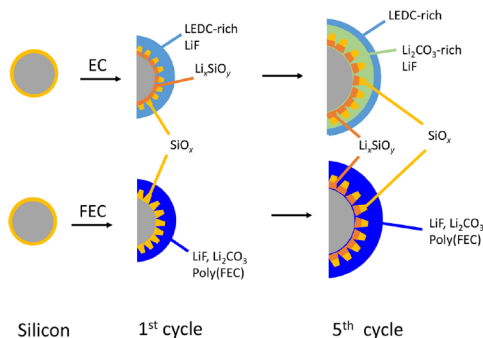
EC – SEI contains LEDC-rich SEI which decomposes but continues to be deposited with cycling

FEC – SEI is mostly poly-FEC with LiF and  $\text{Li}_2\text{CO}_3$  which remains stable with cycling

B.T. Young, et al., "Hard x-ray photoelectron spectroscopy (HAXPES) investigation of the silicon solid electrolyte interphase (SEI) in lithium-ion batteries," *ACS Appl. Mater. Interfaces* **7**, 20004-20011 (2015).

# HAXPES of Si anodes

Using HAXPES data from Si, C, and F, a picture of SEI evolution dependence on electrolyte emerges



as SEI grows, there is growth of  $\text{Li}_x\text{SiO}_y$  underneath as product of lithiation/delithiation

EC – SEI contains LEDC-rich SEI which decomposes but continues to be deposited with cycling

FEC – SEI is mostly poly-FEC with LiF and  $\text{LiCO}_3$  which remains stable with cycling

The FEC acts to stabilize the SEI composition and prevent the change with depth that occurs with EC.

B.T. Young, et al., "Hard x-ray photoelectron spectroscopy (HAXPES) investigation of the silicon solid electrolyte interphase (SEI) in lithium-ion batteries," *ACS Appl. Mater. Interfaces* **7**, 20004-20011 (2015).





# Today's outline - April 02, 2020 (part B)

## Today's outline - April 02, 2020 (part B)

- Final presentations

## Today's outline - April 02, 2020 (part B)

- Final presentations
- Final project (GU Proposal)

## Today's outline - April 02, 2020 (part B)

- Final presentations
- Final project (GU Proposal)

Final Exam (presentations)

Official schedule: Tuesday, May 5, 2020 – 17:00-19:00

Proposed schedule: Tuesday, May 5, 2020 – 15:00 CDT

# Final projects & presentations

In-class student presentations on research topics

# Final projects & presentations

In-class student presentations on research topics

- Choose a research article which features a synchrotron technique

# Final projects & presentations

In-class student presentations on research topics

- Choose a research article which features a synchrotron technique
- Get it approved by instructor first!



# Final projects & presentations

In-class student presentations on research topics

- Choose a research article which features a synchrotron technique
- Get it approved by instructor first!
- Schedule a 15 minute time on Final Exam Day (tentatively, Tuesday, May 5, 2020, 15:00-19:00)

# Final projects & presentations

In-class student presentations on research topics

- Choose a research article which features a synchrotron technique
- Get it approved by instructor first!
- Schedule a 15 minute time on Final Exam Day (tentatively, Tuesday, May 5, 2020, 15:00-19:00)

Final project - writing a General User Proposal

# Final projects & presentations

In-class student presentations on research topics

- Choose a research article which features a synchrotron technique
- Get it approved by instructor first!
- Schedule a 15 minute time on Final Exam Day (tentatively, Tuesday, May 5, 2020, 15:00-19:00)

Final project - writing a General User Proposal

- Think of a research problem (could be yours) that can be approached using synchrotron radiation techniques

# Final projects & presentations

In-class student presentations on research topics

- Choose a research article which features a synchrotron technique
- Get it approved by instructor first!
- Schedule a 15 minute time on Final Exam Day (tentatively, Tuesday, May 5, 2020, 15:00-19:00)

Final project - writing a General User Proposal

- Think of a research problem (could be yours) that can be approached using synchrotron radiation techniques
- Make proposal and get approval from instructor before starting

# Final projects & presentations

In-class student presentations on research topics

- Choose a research article which features a synchrotron technique
- Get it approved by instructor first!
- Schedule a 15 minute time on Final Exam Day (tentatively, Tuesday, May 5, 2020, 15:00-19:00)

Final project - writing a General User Proposal

- Think of a research problem (could be yours) that can be approached using synchrotron radiation techniques
- Make proposal and get approval from instructor before starting
- **Must be different technique than your presentation!**

